

MLLM-For3D: Adapting Multimodal Large Language Model for 3D Reasoning Segmentation

Jiaxin Huang¹ Runnan Chen^{2,†} Ziwen Li¹ Zhengqing Gao¹ Xiao He⁴ Yandong Guo⁴
Mingming Gong³ Tongliang Liu^{2,†}

¹MBZUAI ²The University of Sydney ³The University of Melbourne ⁴AI2Robotic

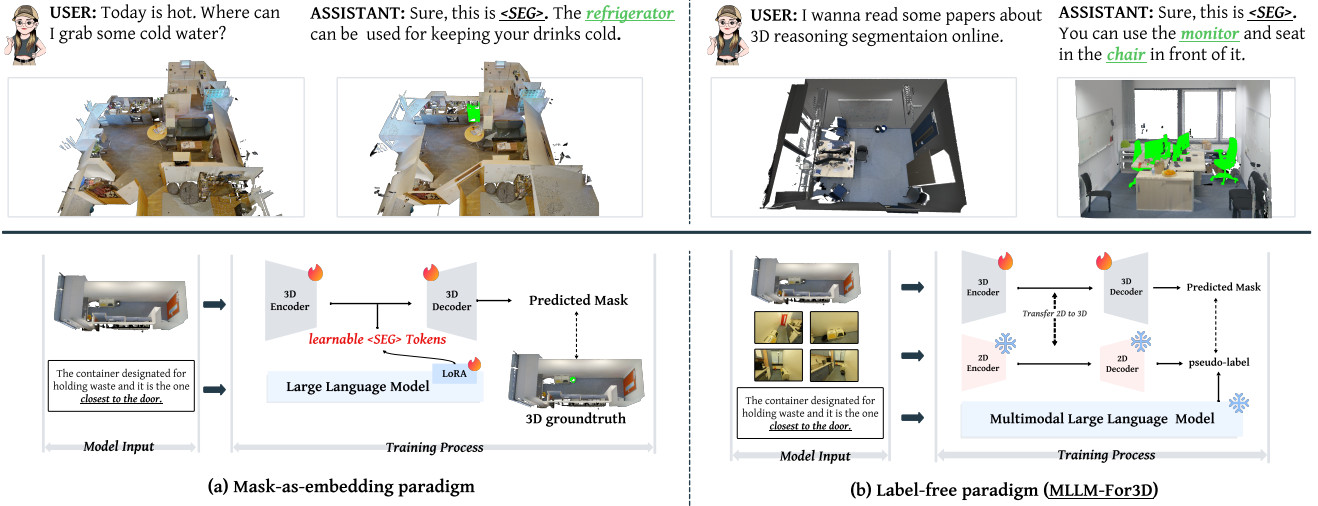


Figure 1. 3D reasoning segmentation interprets implicit user instructions to segment 3D scenes. Our **MLLM-For3D** framework adapts multimodal large language models (MLLMs) to 3D reasoning in a label-free manner, contrasting with the mask-as-embedding paradigm that relies on labeled 3D-text data. By leveraging multi-view images, point clouds, and textual queries, MLLM-For3D infers object masks without manual 3D annotations.

Abstract

Reasoning segmentation aims to segment target objects in complex scenes based on human intent and spatial reasoning. While recent multimodal large language models (MLLMs) have demonstrated impressive 2D image reasoning segmentation, adapting these capabilities to 3D scenes remains underexplored. In this paper, we introduce **MLLM-For3D**, a simple yet effective framework that transfers knowledge from 2D MLLMs to 3D scene understanding. Specifically, we utilize MLLMs to generate multi-view pseudo segmentation masks and corresponding text embeddings, then unproject 2D masks into 3D space and align them with the text embeddings. The primary challenge lies

in the absence of 3D context and spatial consistency across multiple views, causing the model to hallucinate objects that do not exist and fail to target objects consistently. Training the 3D model with such irrelevant objects leads to performance degradation. To address this, we introduce a spatial consistency strategy to enforce that segmentation masks remain coherent in the 3D space, effectively capturing the geometry of the scene. Moreover, we develop a Token-for-Query approach for multimodal semantic alignment, enabling consistent identification of the same object across different views. Extensive evaluations on various challenging indoor scene benchmarks demonstrate that, even without any labeled 3D training data, **MLLM-For3D** outperforms existing 3D reasoning segmentation methods, effectively interpreting user intent, understanding 3D scenes, and reasoning about spatial relationships.

† denotes the corresponding authors.

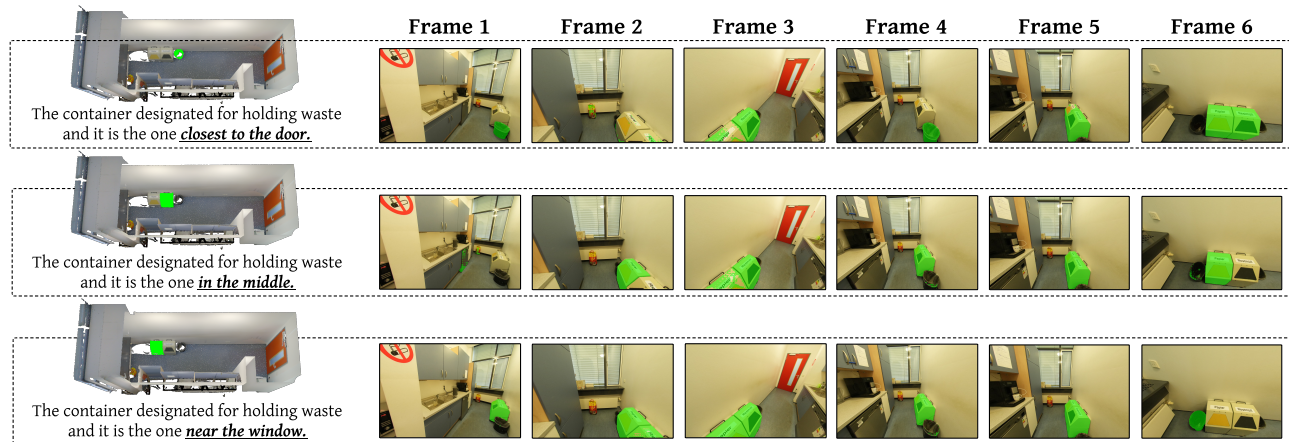


Figure 2. For the same scene, we present three different queries and display the 2D reasoning segmentation results on the same set of frames, illustrating how the model responds to varying instructions.

1. Introduction

Understanding user intent and reasoning about 3D spatial context are crucial for real-world vision applications, including embodied AI, autonomous driving, and augmented/virtual reality. Recent advancements in 3D scene understanding, particularly in multimodal learning [9, 11, 19–21, 39, 55], have spurred the development of 3D point cloud-based Large Language Models (3D-LLMs). These methods allow systems to infer implicit goals, localize objects in complex environments, and interact seamlessly with users. Compared to conventional segmentation, reasoning segmentation poses a more complex challenge, requiring deeper levels of semantic understanding and the ability to handle underspecified or context-dependent queries.

The concept of reasoning segmentation was first introduced in the 2D domain by LISA [31], which employed the mask-as-embedding paradigm to fine-tune large language models using abundant $\langle 2D, 3D \rangle$ paired data. Building upon its success in 2D domains, initial attempts have been made to adapt this paradigm to 3D tasks [18, 22, 27]. However, these approaches have the prohibitive cost of generating high-quality $\langle 3D, text \rangle$ pairs, which often involve labour-intensive manual annotation or computationally expensive synthesizing (e.g., via GPT-4) [1]. A natural question thus arises: *Given a 3D point cloud accompanied by multiple posed RGB views, can we exploit pre-trained 2D reasoning segmentation models to approximate 3D labels?*

Our pilot study illustrates both the promise and the limitations of the idea (Figure 2). We evaluate the performance of 2D reasoning segmentation models, LISA [31] on the ScanNet++ dataset [51], by providing the model with different views corresponding to a 3D scene along with an implicit language instruction. Each frame is processed independently, generating both a reasoning response and a 2D

binary segmentation mask. Ideally, the model should consistently localize the target object across all frames and infer its spatial relationships (e.g., nearest door) within the scene. However, as shown in Figure 2, there are two key limitations of 2D models reasoning in 3D: (i) *False positives in invisible views*: A 2D MLLM processing a single view might hallucinate or mistakenly segment objects that are described by the instruction but not visible in that particular view. Without 3D awareness, the model cannot distinguish between visible and occluded target objects, leading to incorrect mask predictions on some views. (ii) *Multi-View prediction inconsistency* occurs when the model lacks a mechanism to ensure spatial alignment of predictions across views, thereby degrading the performance when we aggregate multi-view predictions into 3D.

In this paper, we introduce **MLLM-For3D**, a simple yet effective framework that transfers 2D MLLM reasoning capabilities to 3D scene understanding. Specifically, we use a pre-trained MLLM to generate multi-view pseudo segmentation masks and corresponding text embeddings. These masks are then unprojected into 3D space and aligned with the textual information to supervise the learning of the 3D model, eliminating the need for explicit 3D annotations. To address the critical issue of cross-view inconsistencies, we incorporate a **spatial consistency strategy** into the mask generation process, ensuring that the latent space remains coherent and mitigating object hallucinations. Specifically, we enforce latent space consistency by aggregating the per-view predictions via an attention-based fusion module. In this module, for a given 3D point visible in multiple views, each view’s contribution is weighted by its reliability and its semantic similarity to a unified query vector derived from the [SEG] token embeddings. Furthermore, we propose a **Token-for-Query** mechanism that consistently binds the

same object identity across different views, enhancing the 3D model’s ability to interpret implicit user instructions and reason about spatial relationships.

MLLM-For3D is evaluated on three challenging benchmarks and shows that it achieves state-of-the-art performance in 3D reasoning segmentation tasks even without the need for any 3D annotations, which achieves about 55% higher mIoU than the previous methods. By effectively transferring 2D MLLM reasoning capabilities to 3D, our framework exhibits strong robustness to ambiguous queries, improved spatial reasoning, and superior segmentation performance.

The contributions are as follows:

- We propose a simple yet effective framework to adapt 2D MLLMs for 3D reasoning segmentation, eliminating the need for manual 3D annotations.
- We integrate a spatial consistency strategy to refine multi-view pseudo segmentation masks, reducing the presence of hallucinated objects across frames.
- We introduce a novel alignment mechanism that binds token embeddings to specific queries, ensuring consistent segmentation of the same object across views.
- Extensive evaluations on two challenging indoor scene benchmarks demonstrate that MLLM-For3D outperforms existing 3D reasoning segmentation methods, even without any 3D labeled training data.

2. Related Work

2.1. Reasoning Segmentation

Reasoning segmentation is first introduced by LISA [31], which integrates a multimodal LLM (e.g., LLaVA [33]) with the Segmentation Anything Model (SAM) [30] to handle complex and *implicit* instructions in 2D images. PixelLM [42] builds on this paradigm by adopting a lightweight decoder and segmentation codebook for multi-object reasoning segmentation. LLM-Seg [45] uses SAM to propose candidate masks and lets the LLM reason which mask fits the query. VISA [47] and VideoLISA [2] extend these approaches to video data, addressing temporal coherence and object tracking. FAST [43], an agent-based pipeline, further refines segmentation masks by iteratively identifying and masking key objects. These advancements in 2D demonstrate the value of combining segmentation with LLM reasoning: models can interpret rich instructions and produce the corresponding mask, which is not possible with traditional segmentation alone.

In 3D Domains, PARIS3D [29] and Reasoning3D [10] focus on part segmentation with explanatory capabilities for individual objects, leaving scene-level reasoning tasks relatively unexplored. More recently, Segpoint [18], Reason3D [22], and MORE3D [27] have adapted LISA’s embedding-as-mask paradigm, aiming to unify multiple

3D tasks through human-like instructions. Despite their success, these methods typically require extensive 3D-text training data generated by GPT-4 [1] and end-to-end fine-tuning of LLMs, both of which are computationally costly. In contrast, our approach alleviates this problem by distilling both reasoning capabilities and semantic information from 2D MLLMs into a 3D, enabling label-free 3D reasoning segmentation.

2.2. Label-Free 3D Scene Understanding

Open-Vocabulary and Zero-Shot Approaches. To alleviate the annotation burden, several label-free scene understanding methods leverage *vision foundation models* for zero-shot 3D segmentation [4, 6–8, 15, 17, 25, 32, 35, 37, 38, 52]. OpenScene [38] employs 2D open-vocabulary segmentors [17, 32] to align pixel-level embeddings with 3D points, enabling object category recognition for unseen classes. CLIP2Scene [6] employs MaskCLIP [54] to obtain pixel-aligned features for annotation-free and label-efficient scene understanding. ConceptFusion [25] and CLIP-FO3D [52] further explore acquiring pixel-aligned knowledge through dense region-level feature extraction using CLIP [40] and multi-view feature fusion. PLA [15] proposed a language-driven 3D scene understanding paradigm, which obtains point-language paired data through image captioning by visual-language foundation models for training 3D backbones. Similarly, RegionPLC [50] and Lowis3D [16] build point-caption pairs by projecting 2D visual-language features onto 3D geometry. Methods like OVIR3D [36] and MaskClustering [48] merge zero-shot 2D masks with 3D semantics for instance segmentation. Recent efforts [5, 26] also combine different foundation models (e.g., LLaVa-1.5 [33] and SEEM [56]) to unify zero-shot 2D embeddings and 3D voxel/point features, demonstrating strong category expansion in 3D.

Label-Free 3D Reasoning Segmentation. While these label-free strategies effectively handle open-vocabulary classes, their prompts remain relatively straightforward, limiting their ability to interpret more nuanced or context-heavy queries. In this work, we target *implicit* user prompts requiring both semantic and spatial comprehension. Our framework, **MLLM-For3D**, inherits the reasoning capabilities of LISA and applies them to 3D *without direct 3D annotations*, making it both *scalable* and *intuitive* in real-world scenarios.

3. Methodology

We propose **MLLM-For3D**, a framework that adapts 2D multimodal large language models (MLLMs) for 3D reasoning segmentation by transferring knowledge from 2D to the 3D domain as shown in Figure 3. Our approach integrates multi-view RGB frames, corresponding 3D point clouds, and implicit descriptions to generate pseudo-labels

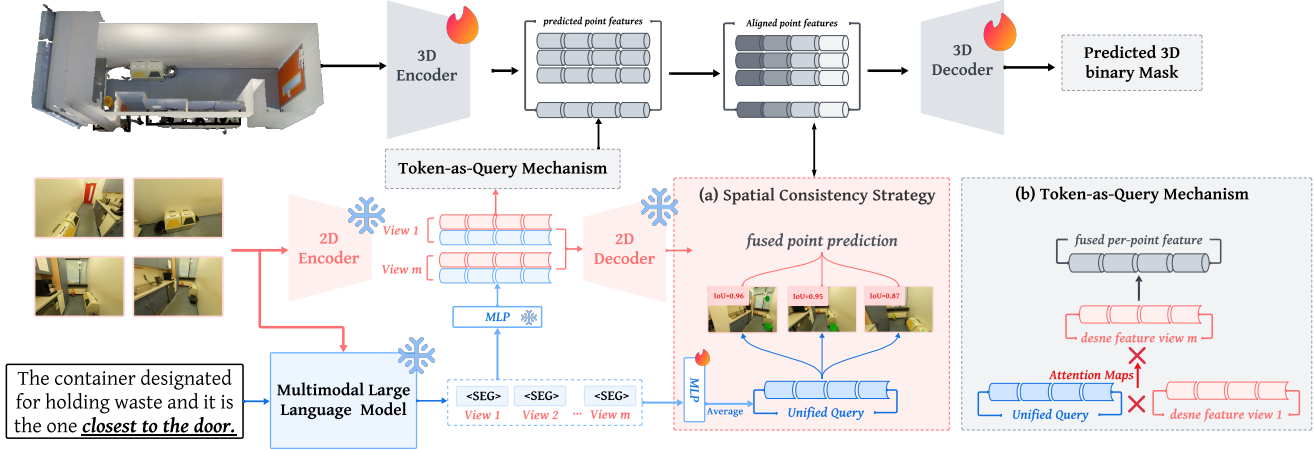


Figure 3. Overview of the proposed **MLLM-For3D** framework. We adapt multimodal large language models (MLLMs) for 3D reasoning segmentation by generating multi-view pseudo-labels from 2D masks and enforcing cross-view consistency via a spatial consistency strategy. Additionally, a *Token-for-Query* mechanism aligns 2D [SEG] token embeddings with 3D point features, enabling consistent object identity binding across views. Leveraging multi-view images, point clouds, and textual instructions, our method produces 3D pseudo-labeled masks without manual annotations, effectively transferring 2D knowledge into a 3D backbone.

for 3D segmentation without requiring manually annotated 3D masks. Specifically, we use a pre-trained 2D MLLM along with a segmentation model to segment target objects in posed images and propagate these pseudo segmentation masks into 3D via geometric consistency constraints.

Despite their strong per-frame segmentation performance, pre-trained 2D models often struggle with spatial consistency across views. Consequently, the model often *hallucinates* target objects that do not exist in some images and fails to identify the same object cross-views, thereby degrading the performance when we aggregate multi-view predictions into 3D. To mitigate these challenges, we introduce (1) a spatial consistency strategy that enforces geometric coherence across views and (2) a *Token-for-Query* mechanism that aligns multimodal information by leveraging shared embeddings between textual descriptions and segmentation features.

3.1. Pseudo-Label Generation

A cornerstone of our methodology is the absence of any human-labeled 3D ground-truth masks. Instead, we adapt a pre-trained 2D MLLM and a segmentation model to act as a pseudo-label generator for 3D data. Concretely, for each 3D point cloud $\mathbf{P} \in \mathbb{R}^{M \times 3}$ with M points, we have m posed multi-view frames $\{I_i\}_{i=1}^m$ of resolution $H \times W$, along with n textual descriptions $\{X_j\}_{j=1}^n$ conveying user intent. For each view I_i and each description d_j , we employ the MLLM to generate a [SEG] token embedding $\mathbf{Y}_{ij} \in \mathbb{R}^d$. This embedding is then used as a prompt for a frozen 2D segmentation model (e.g., SAM). In particular, SAM extracts a dense feature map $\mathbf{F}_i^{2D} \in \mathbb{R}^{H' \times W' \times C}$ from the image encoder, and its mask decoder produces a binary mask

$M_{ij}^{2D} \in \{0, 1\}^{H \times W}$ along with a quality score (IoU) κ_{ij} .

Point-Pixel Pairing. To propagate 2D segmentation into 3D, we follow the point-pixel correspondences proposed by [6] to unproject each mask M_{ij}^{2D} into the shared 3D space. Specifically, if $M_i(u_i) = 1$ for pixel u_i (indicating that u_i lies inside the mask in view i), then view i “votes” that the corresponding 3D point X belongs to the target segment; otherwise, view i votes negative. Repeating this for all views yields multiple predicted labels per 3D point, forming the basis for our subsequent cross-view fusion.

3.2. Spatial Consistency Strategy

While pseudo-labels derived from 2D segmentation can be informative, single-view predictions may conflict across different viewpoints. We introduce an attention-based fusion module that combines per-view segmentation results, assigning weights that reflect each view’s reliability and semantic relevance.

Unified Query. First, we derive a unified query vector Q to capture the overall instruction semantics in a view-independent manner. Concretely, we take each view’s [SEG] token embedding \mathbf{p}_i and average them to obtain Q , representing the aggregated textual intent.

Attention-Like Weighting. For each view i , we then compute a weight w_i that factors in: (1) the mask confidence κ_i from SAM’s decoder, and (2) the similarity between \mathbf{p}_i and Q . Formally,

$$w_i = \frac{\kappa_i \exp(\text{sim}(\mathbf{p}_i, Q))}{\sum_{j \in V_P} \kappa_j \exp(\text{sim}(\mathbf{p}_j, Q))},$$

where $\text{sim}(\mathbf{p}_i, Q)$ is the dot product in a shared latent space,

and V_P denotes the set of views in which point P is visible. This weighting favors views that produce high-quality masks (large κ_i) and that align well with the unified query while penalizing views with low-quality or off-target predictions.

Fused Prediction & Consistency. Using these weights w_i , we aggregate multi-view predictions into a single consensus. For point P , the fused probability is:

$$p_{\text{fused}}(P) = \sum_{i \in V_P} w_i p_i(P).$$

We then apply a spatial consistency loss that penalizes disagreements among per-view predictions ($p_i(X)$) and their fused result ($p_{\text{fused}}(X)$). Specifically, we combine an alignment term $\mathcal{L}_{\text{align}}^{3D}$ (which enforces consistency across views) with an attention-fusion term $\mathcal{L}_{\text{spatial}}$ (which ensures $p_i(X)$ is close to $p_{\text{fused}}(X)$). Merging these into a multi-view consistency objective encourages the model to learn a representation that is invariant to single-view noise and accurately reflects true 3D geometry and semantics. This loss term guides the network to find a latent representation where the segmentation decision is view-invariant, relying on true 3D geometry and semantics rather than view-specific cues.

3.3. Multimodal Semantic Alignment

Token-for-Query Mechanism. To solve the inconsistency of object segmentation across views, we develop an attention-based token-for-query mechanism that unifies multi-view features into a single 3D representation. We leverage the same query vector Q , while the 2D dense features from each view serve as keys and values in an attention mechanism.

For each 3D point X , let $\mathbf{f}_i(X) \in \mathbb{R}^d$ be the local feature extracted from the i -th view’s dense feature map at pixel $u_i = \Pi_i(X)$. We compute attention weights by comparing each $\mathbf{f}_i(X)$ to Q :

$$\alpha_i(X) = \frac{\exp(Q \cdot \mathbf{f}_i(X))}{\sum_{j \in V_X} \exp(Q \cdot \mathbf{f}_j(X))},$$

where V_X is the set of views where point X is observed. The fused 3D feature is

$$\mathbf{F}^{3D}(X) = \sum_{i \in V_X} \alpha_i(X) \mathbf{f}_i(X).$$

Intuitively, Q “queries” each view for features relevant to the user’s instruction, and $\mathbf{F}^{3D}(X)$ consolidates them into a single descriptor.

This token-for-query mechanism ensures that only features pertinent to the query concept are emphasized across views, naturally achieving semantic alignment. Because special Q attends to all views, disparate viewpoints yield

a coherent representation when focusing on the same object. This greatly enhances the reasoning capabilities of the 3D model. For example, if one view only partially sees the object, another view can provide missing details through attention, and Q will fuse these into a complete understanding of the point X . In summary, Q gathers and unifies multi-view visual information, allowing the model to reason about the 3D scene at a higher level of abstraction than individual images.

3.4. Implicit Inference

By training with these pseudo-labels and enforcing both spatial consistency and token-based attention, we obtain a 3D segmentation model that generalizes effectively to new scenes. At inference time, given multi-view images and implicit instruction, our model produces a coherent 3D segmentation without requiring any 3D manual annotations. This paradigm effectively transfers the rich 2D multimodal knowledge into 3D, enabling label-free 3D reasoning segmentation.

4. Experiments

This section presents the experimental results for three challenging tasks, focusing on reasoning segmentation. For the *3D reasoning segmentation* task, we adopt Instruct3D [18] as benchmarks, which is derived from ScanNet++ [51], which retains only *nearly complete* 3D instances. After filtering, the dataset is split into 136 scenes for training and 45 for validation, yielding 1,034 and 321 question-answer pairs, respectively. Due to the limited open-source evaluation datasets in this area, we try to evaluate our method on similar tasks like 3D intention grounding (3D-IG) [28] and grounding benchmarks without object names (VG-w/o-ON) [46]. These two datasets are built on ScanNet [13], leveraging its scene annotations for evaluation. Implementation details, additional experiments, and qualitative results are provided in the supplementary material.

4.1. Main Results

3D Reasoning Segmentation. Instruct3D is derived from ScanNet++ [51], which retains only *nearly complete* 3D instances. Removing explicit instructions and annotations from Instruct3D makes the task much harder since models can no longer rely on direct object names or step-by-step instructions and must infer the user’s intent from implicit hints. After filtering, the dataset is split into 136 scenes for training and 45 for validation, yielding 1,034 and 321 question-answer pairs, respectively.

As shown in Table 1, MLLM-For3D shows significant gains in 3D reasoning segmentation accuracy over Reason3D on the filtered Instruct3D [18] benchmark. Removing explicit instructions and annotations from Instruct3D makes the task much harder since models can no longer

rely on direct object names or step-by-step instructions and must infer the user’s intent from implicit hints. In this setting, MLLM-For3D achieves about 15% higher Acc@0.25 and 10% higher Acc@0.50 than Reason3D. It also improves mean IoU by 10 points, indicating more precise mask predictions. These improvements highlight MLLM-For3D’s stronger reasoning capability: it can understand complex or implicit instructions to segment the correct 3D regions even when keywords are missing. In contrast, the Reason3D baseline struggles without explicit instructions since it was designed to output masks based on more direct textual descriptions. Overall, MLLM-For3D’s ability to interpret implicit instructions leads to better performance in the 3D reasoning segmentation task.

VG-w/o-ON: Spatial Reasoning without Object Names

In the 3D visual grounding without object names task, MLLM-For3D achieves state-of-the-art results as shown in Table 2, outperforming the EDA baseline and others. VG-w/o-ON is a particularly challenging benchmark variant where the language query describes spatial relationship of the target object without naming it explicitly. Conventional 3D referring models struggle here since they typically rely on matching object names in the query. Indeed, we observe drastic drops in baseline performance: methods like ScanRefer [3] and TGNN [23] see their accuracy plunge to nearly chance level (e.g., 10% success) when object names are missing. Even EDA [46] reaches only 26.5% Acc@0.25 and 21.6% Acc@0.50 when object names are missing, much lower than on normal queries. MLLM-For3D overcomes this limitation by using the query’s descriptive and contextual instructions to infer the target. It delivers roughly 12–13% higher Acc@0.25 and 8–9% higher Acc@0.50 than EDA on the VG-w/o-ON benchmark, along with a notable improvement in mIoU.

Such results denotes that our approach is capable of spatial reasoning by connect the spatial relationship to the correct object in space. This contextual reasoning allows it to maintain high grounding accuracy despite the missing noun, whereas methods like EDA falter because they try to decompose the sentence and end up misled or unsure without an explicit object name. By leveraging the abundant semantic information of a 2D MLLM, MLLM-For3D fills in the semantic gaps (the missing object names) with informed guesses and uses the 3D visual input to confirm those guesses. This results in superior grounding performance under this no-name condition. We will then discuss in the ablation study how our proposed spatial consistency enhances the spatial reasoning ability.

3D Intention Grounding (3D-IG). On the Intent3D dataset for the 3D intention grounding task, MLLM-For3D outperforms the specialized IntentNet [28], which requires detecting the object that fulfills an implicit human intention (e.g. “I want something to support my back” implies “pil-

3D Reasoning Segmentation Methods	Venue	Modality	Instruct3D (val)		
			Acc@0.25	Acc@0.50	mIoU
<i>LLM Agent-based Model</i>					
LLM-Grounder [†] [49]	[ICRA’24]	3D	23.7	15.6	17.2
<i>LLM-based Model (w/ label)</i>					
TGNN [*] [23]	[AAAI’22]	3D	4.76	4.76	3.51
Reason3D [†] [22]	[3DV’25]	3D	18.35	10.55	12.43
<i>MLLM-based Model (w/ label)</i>					
LISA-7B (MLLM-For3D)	-	3D+2D	45.5	38.7	31.9
LISA-13B (MLLM-For3D)	-	3D+2D	46.7	39.0	32.3
VideoLISA (MLLM-For3D)	-	3D+2D	48.2	40.4	34.5
<i>MLLM-based Model (w/o label)</i>					
LISA-7B (MLLM-For3D)	-	3D+2D	39.1	29.7	23.9
LISA-13B (MLLM-For3D)	-	3D+2D	40.9	30.5	26.4
VideoLISA (MLLM-For3D)	-	3D+2D	41.0	32.1	28.2

Table 1. **Evaluation of 3D Reasoning Segmentation on Instruct3D [18] (val).** Our method achieves state-of-the-art performance with both label-free and labeled settings. † indicates that we re-trained TGNN, Reason3D using the filters Instruct3D training set for a fair comparison on this benchmark.

Methods	Venue	Acc@0.25 [†]	Acc@0.50 [†]	mIoU [†]
<i>LLM-based Model (w/ label)</i>				
ScanRefer [3]	[ECCV’20]	10.51	6.20	-
TGNN [*] [23]	[AAAI’21]	11.64	9.51	8.13
InstanceRefer [36]	[ICCV’21]	13.92	11.47	-
BUTD-DETR [24]	[ECCV’22]	11.99	8.95	-
M3DRef-CLIP [53]	[ICCV’23]	18.3	14.8	10.29
EDA [46]	[CVPR’23]	26.50	21.20	-
Reason3D [†] [22]	[3DV’25]	17.64	13.11	13.05
IntentNet [28]	[ICLR’25]	28.12	22.63	18.92
<i>MLLM-based Model (w/ label)</i>				
LISA-7B (MLLM-For3D)	-	31.88	29.90	28.10
LISA-13B (MLLM-For3D)	-	32.52	30.15	29.81
VideoLISA (MLLM-For3D)	-	33.12	31.21	30.45
<i>MLLM-based Model (w/o label)</i>				
LISA-7B (MLLM-For3D)	-	26.49	22.12	21.05
LISA-13B (MLLM-For3D)	-	27.31	24.49	23.93
VideoLISA (MLLM-For3D)	-	<u>29.50</u>	<u>25.61</u>	<u>24.28</u>

Table 2. **Evaluation results on VG-w/o-ON (val) evaluated by Acc and mIoU;** * auxiliary mask head. † indicates that we re-trained Reason3D using the ScanRefer[3] training set for a fair comparison on this benchmark.

low” on a chair). This is challenging because the target object’s name may never be mentioned explicitly. IntentNet, a task-specific model, achieves 41.9% AP@0.25 and 25.4% AP@0.50 on this benchmark. MLLM-For3D surpasses this with 6–7 point higher AP@0.25 and 5 point higher AP@0.50 (as well as a 7% absolute gain in mIoU), indicating it more reliably identifies the correct object from just the implied intent.

For further comparison shown in Table 3, our method *MLLM-For3D* is evaluated under two settings: (i) with labeled 3D-text data (pink rows) and (ii) without labels (yellow rows). Despite the absence of manual 3D annotations in the label-free setting, our model surpasses the specialized IntentNet[28] by a notable margin. For in-

3D Intention Grounding Methods	Venue	Modality	LLM/MLLM Backbone	Intent3D (val)				
				Top1-Acc@0.25	Top1-Acc@0.50	AP@0.25	AP@0.50	mIoU
<i>LLM-based Model</i>								
BUTD-DETR [24]	[ECCV'22]	3D	RoBERTa [34]	47.12	24.56	31.05	13.05	-
EDA [46]	[CVPR'23]	3D	RoBERTa [34]	43.11	18.91	14.02	5.00	-
3D-VisTA [55]	[ICCV'23]	3D	BERT [14]	42.76	30.37	36.1	19.93	-
Chat-3D-v2 ⁰ [20]	[NIPS'24]	3D+2D	Vicuna-7B [44]	5.86	5.24	0.15	0.13	-
Chat-Scene [20]	[NIPS'24]	3D+2D	Vicuna-7B [44]	36.71	32.78	3.23	2.58	-
IntentNet [28]	[ICLR'25]	3D	RoBERTa [34]	58.34	40.83	41.90	25.36	-
Reason3D [†] [22]	[3DV'25]	3D	Flan-T5[12]	-	-	61.71	51.68	47.30
<i>MLLM-based Model (w/ label)</i>								
LISA-7B (MLLM-For3D)	-	3D+2D	LLaVA-2	-	-	57.31	47.92	42.98
LISA-13B (MLLM-For3D)	-	3D+2D	LLaVA-2	-	-	58.40	48.75	44.13
VideoLISA (MLLM-For3D)	-	3D+2D	LLaVA-Phi-3-V [41]	-	-	<u>59.90</u>	<u>50.01</u>	<u>45.18</u>
<i>MLLM-based Model (w/o label)</i>								
LISA-7B (MLLM-For3D)	-	3D+2D	LLaVA-2	-	-	48.24	39.61	34.53
LISA-13B (MLLM-For3D)	-	3D+2D	LLaVA-2	-	-	49.92	40.10	35.75
VideoLISA (MLLM-For3D)	-	3D+2D	LLaVA-Phi-3-V [41]	-	-	50.89	41.56	36.92

Table 3. **Evaluation of 3D Intention Grounding on the Intent3D [28] validation set.** The best results are in **bold**, and the second-best results are underlined. † indicates that we re-trained Reason3D using the Intent3D training set for a fair comparison on this benchmark. The color gradient reflects different model backbones in MLLM-For3D.

stance, comparing the best label-free variant **VideoLISA (MLLM-For3D)** with IntentNet, we observe an improvement of +9.0 points on AP@0.25 (41.90% → 50.89%) and +16.2 points on AP@0.50 (25.36% → 41.56%). This indicates that a multimodal LLM can better interpret diverse intention phrases and incorporate broader world knowledge than a system trained on fixed detection templates. Meanwhile, Reason3D [22] remains slightly ahead of our approach. We attribute this gap to Reason3D’s mask-as-embedding paradigm, which excels at implicit intent reasoning by leveraging large language models for direct segmentation tokens. Nonetheless, *MLLM-For3D* still demonstrates strong generalization across intent expressions, effectively combining detection and segmentation reasoning in a label-free manner. In contrast, IntentNet is tailored primarily for detection, and Reason3D focuses on search-plus-segmentation. Our method’s multimodal design instead offers a more balanced approach, achieving second-best results while using no 3D labels.

4.2. Visual Comparisons

Figure 4 presents qualitative examples comparing our **MLLM-For3D** framework against a previous state-of-the-art baseline on 3D reasoning segmentation tasks. Each row shows the ground-truth rendered scene, the predicted mask from the baseline, our result, and the text query. In the first example (left two columns), for the instruction “The container designated for holding waste and it is the one closest to the door”, the baseline incorrectly merges multiple objects or fails to capture the target, whereas **MLLM-For3D** precisely identifies only the correct container. In another

example (right columns), given “If you want to let in natural light and fresh air once the air starts at night, which part of the room would you open?”, the baseline misses key portions under occlusion, while our approach segments the relevant object more completely. These comparisons show that our model follows high-level instructions more faithfully, resolving common failure modes (e.g., mixing up object types or ignoring occluded areas) by leveraging LLM-driven 3D reasoning.

4.3. Ablation studies & Analysis

We conduct extensive ablations to verify each component’s contribution. The quantitative results are shown in Table 4.

(a) 2D Projection Baseline: First, we compare against a baseline that applies a 2D reasoning segmentation model to 3D scenes by projection. We unproject the multi-view masks generated by LISA-7B back to the point cloud. This naive approach yields much lower accuracy – roughly 50% lower mIoU – than our full 3D method. The projected baseline often produces incomplete or misaligned segmentations since each view sees only part of the scene without cross-view consistency enforcement. This highlights the importance of reasoning directly in 3D rather than per-view 2D.

(b) Spatial Consistency Module: Next, we ablate the multi-view spatial alignment module. Disabling this module (so that each view is processed independently) leads to inconsistent masks and a drop of 2-4% in segmentation accuracy. Enforcing spatial consistency across views improves performance: by aligning features in 3D space, the model learns a unified segmentation that is viewpoint-invariant, resolving ambiguities from single perspectives.

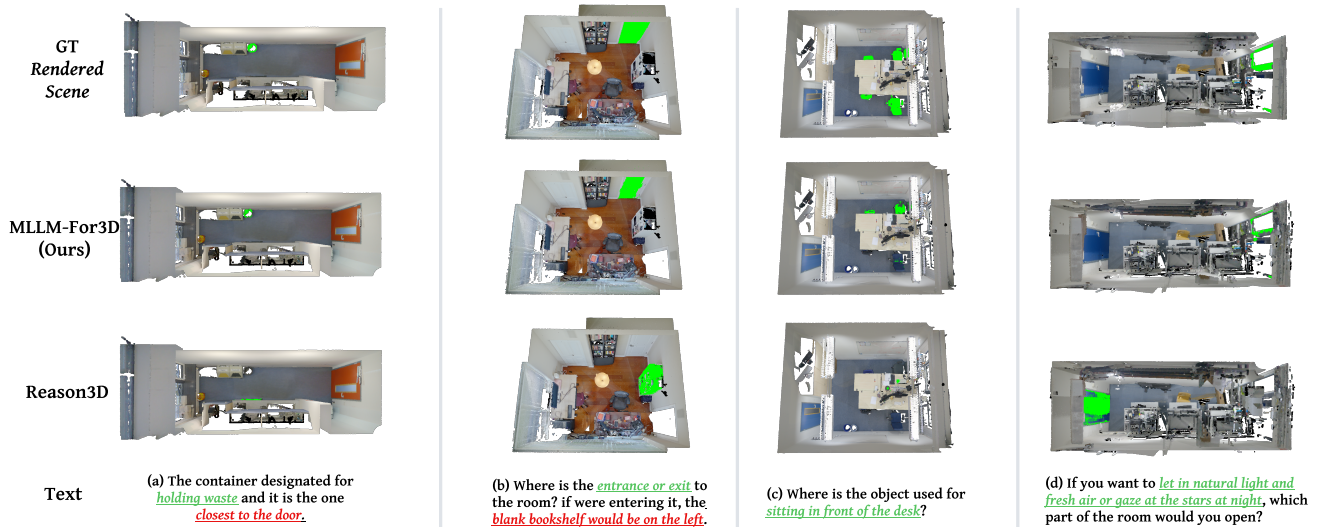


Figure 4. **Qualitative comparisons of our MLLM-For3D versus a previous state-of-the-art method.** For each row, we show the ground-truth rendered scene (left), the baseline’s prediction, our result, and the textual query. Our method accurately interprets implicit user instructions and produces coherent 3D masks, even under challenging scenarios like occlusion or ambiguous references.

Ablation Study	$+\mathcal{L}_{\text{spatial}}$	$+\mathcal{L}_{\text{semantic}}$	Intent3D (val)			VG-w/o-ON (val)		
			Acc@0.25	Acc@0.50	mIoU	Acc@0.25*	Acc@0.50*	mIoU*
(a) Baseline			29.25	25.26	19.75	20.2	17.24	11.56
(b) Spatial Consistency	✓		34.53	28.75	21.02	23.2	19.1	18.48
(c) Token-for-Query		✓	33.92	28.53	20.93	24.5	20.7	19.92
(d) Full Configuration	✓	✓	39.1	29.7	23.9	26.49	22.12	21.05

Table 4. Ablation study evaluating the effectiveness of each proposed component on the Intent3D and VG-w/o-ON validation sets. The best results are in **bold**.

(c) Token-for-Query Mechanism: We examine the impact of our query-specific token design, which assigns a unique token embedding for each textual query for semantic alignment guidance. Removing this mechanism causes a notable uptick in false positives – the model sometimes activates multiple objects or unrelated regions for a single query. With the token-for-query in place, the model focuses on one target at a time, reducing false positives by 30% (and improving mIoU by 2 points). This mechanism ensures one coherent mask per query and consistent segmentation even when multiple queries are issued in one scene.

(d) Backbone Variants: Finally, we also investigate the impact of different model sizes and backbone types. Replacing the smaller LISA-7B with the larger LISA-13B (13B parameters) improves performance by approximately 1–2% on all evaluated benchmarks, indicating that a more expressive language-vision model better interprets complex user instructions. Moreover, incorporating a video-capable backbone (VideoLISA) yields an additional 1.5% improvement on average, suggesting that temporal context further enhances the model’s reasoning ability.

5. Conclusion

We introduce **MLLM-For3D**, a novel framework that adapts MLLMs for 3D reasoning segmentation via a *label-free* paradigm. Our approach tackles challenges such as single-view hallucination and cross-view inconsistencies by employing an attention-based fusion strategy alongside a Token-for-Query mechanism, enabling coherent 3D pseudo-label generation without manual 3D annotations. Experiments on three challenging benchmarks reveal that our method achieves SOTA performance in label-free settings, and demonstrates further improvements when 3D labels are made available. These results confirm the effectiveness of our adaptation strategy and open new avenues for scalable, language-guided 3D scene understanding. However, the method can be computationally demanding, as it involves multiple inferences of 2D MLLMs and a 3D backbone. Future work may explore more efficient architectures, better uncertainty modeling of pseudo-labels, and broader generalization to complex, real-world 3D environments.

References

- [1] Josh Achiam, Steven Adler, Sandhini Agarwal, Lama Ahmad, Ilge Akkaya, Florencia Leoni Aleman, Diogo Almeida, Janko Altenschmidt, Sam Altman, Shyamal Anadkat, et al. Gpt-4 technical report. *arXiv preprint arXiv:2303.08774*, 2023. 2, 3
- [2] Zechen Bai, Tong He, Haiyang Mei, Pichao Wang, Ziteng Gao, Joya Chen, Zheng Zhang, and Mike Zheng Shou. One token to seg them all: Language instructed reasoning segmentation in videos. *NeurIPS*, 37:6833–6859, 2025. 3
- [3] Dave Zhenyu Chen, Angel X Chang, and Matthias Nießner. Scanrefer: 3d object localization in rgb-d scans using natural language. In *ECCV*, pages 202–221. Springer, 2020. 6
- [4] Runnan Chen, Xinge Zhu, Nenglu Chen, Wei Li, Yuexin Ma, Ruigang Yang, and Wenping Wang. Zero-shot point cloud segmentation by transferring geometric primitives. *arXiv preprint arXiv:2210.09923*, 2022. 3
- [5] Runnan Chen, Youquan Liu, Lingdong Kong, Nenglu Chen, Xinge Zhu, Yuexin Ma, Tongliang Liu, and Wenping Wang. Towards label-free scene understanding by vision foundation models. In *NeurIPS*, pages 75896–75910, 2023. 3
- [6] Runnan Chen, Youquan Liu, Lingdong Kong, Xinge Zhu, Yuexin Ma, Yikang Li, Yuenan Hou, Yu Qiao, and Wenping Wang. Clip2scene: Towards label-efficient 3d scene understanding by clip. In *CVPR*, pages 7020–7030, 2023. 3, 4
- [7] Runnan Chen, Xinge Zhu, Nenglu Chen, Wei Li, Yuexin Ma, Ruigang Yang, and Wenping Wang. Bridging language and geometric primitives for zero-shot point cloud segmentation. In *ACM MM*, pages 5380–5388, 2023.
- [8] Runnan Chen, Xiangyu Sun, Zhaoqing Wang, Youquan Liu, Jiepeng Wang, Lingdong Kong, Jiankang Deng, Mingming Gong, Liang Pan, Wenping Wang, et al. Ovgaussian: Generalizable 3d gaussian segmentation with open vocabularies. *arXiv preprint arXiv:2501.00326*, 2024. 3
- [9] Sijin Chen, Xin Chen, Chi Zhang, Mingsheng Li, Gang Yu, Hao Fei, Hongyuan Zhu, Jiayuan Fan, and Tao Chen. Ll3da: Visual interactive instruction tuning for omni-3d understanding reasoning and planning. In *CVPR*, pages 26428–26438, 2024. 2
- [10] Tianrun Chen, Chunan Yu, Jing Li, Jianqi Zhang, Lanyun Zhu, Deyi Ji, Yong Zhang, Ying Zang, Zejian Li, and Lingyun Sun. Reasoning3d-grounding and reasoning in 3d: Fine-grained zero-shot open-vocabulary 3d reasoning part segmentation via large vision-language models. *arXiv preprint arXiv:2405.19326*, 2024. 3
- [11] Yilun Chen, Shuai Yang, Haifeng Huang, Tai Wang, Runsen Xu, Ruiyuan Lyu, Dahua Lin, and Jiangmiao Pang. Grounded 3d-llm with referent tokens. *arXiv preprint arXiv:2405.10370*, 2024. 2
- [12] Hyung Won Chung, Le Hou, Shayne Longpre, Barret Zoph, Yi Tay, William Fedus, Yunxuan Li, Xuezhi Wang, Mostafa Dehghani, Siddhartha Brahma, et al. Scaling instruction-finetuned language models. *Journal of Machine Learning Research*, 25(70):1–53, 2024. 7
- [13] Angela Dai, Angel X. Chang, Manolis Savva, Maciej Halber, Thomas Funkhouser, and Matthias Nießner. Scannet: Richly-annotated 3d reconstructions of indoor scenes. In *CVPR*, 2017. 5
- [14] Jacob Devlin, Ming-Wei Chang, Kenton Lee, and Kristina Toutanova. Bert: Pre-training of deep bidirectional transformers for language understanding. In *Proceedings of the 2019 conference of the North American chapter of the association for computational linguistics: human language technologies, volume 1 (long and short papers)*, pages 4171–4186, 2019. 7
- [15] Runyu Ding, Jihan Yang, Chuhui Xue, Wenqing Zhang, Song Bai, and Xiaojuan Qi. Pla: Language-driven open-vocabulary 3d scene understanding. In *CVPR*, pages 7010–7019, 2023. 3
- [16] Runyu Ding, Jihan Yang, Chuhui Xue, Wenqing Zhang, Song Bai, and Xiaojuan Qi. Lowis3d: Language-driven open-world instance-level 3d scene understanding. *IEEE TPAMI*, 2024. 3
- [17] Golnaz Ghiasi, Xiuye Gu, Yin Cui, and Tsung-Yi Lin. Scaling open-vocabulary image segmentation with image-level labels. In *ECCV*, pages 540–557. Springer, 2022. 3
- [18] Shuting He, Henghui Ding, Xudong Jiang, and Bihan Wen. Segpoint: Segment any point cloud via large language model. In *ECCV*, pages 349–367. Springer, 2024. 2, 3, 5, 6
- [19] Yining Hong, Haoyu Zhen, Peihao Chen, Shuhong Zheng, Yilun Du, Zhenfang Chen, and Chuang Gan. 3d-llm: injecting the 3d world into large language models. In *NeurIPS*, pages 20482–20494, 2023. 2
- [20] Haifeng Huang, Yilun Chen, Zehan Wang, Rongjie Huang, Runsen Xu, Tai Wang, Luping Liu, Xize Cheng, Yang Zhao, Jiangmiao Pang, et al. Chat-scene: Bridging 3d scene and large language models with object identifiers. In *NeurIPS*, 2024. 7
- [21] Jiangyong Huang, Silong Yong, Xiaojian Ma, Xiongkun Linghu, Puhao Li, Yan Wang, Qing Li, Song-Chun Zhu, Baoxiong Jia, and Siyuan Huang. An embodied generalist agent in 3d world. In *ICML*, pages 20413–20451, 2024. 2
- [22] Kuan-Chih Huang, Xiangtai Li, Lu Qi, Shuicheng Yan, and Ming-Hsuan Yang. Reason3d: Searching and reasoning 3d segmentation via large language model. *arXiv preprint arXiv:2405.17427*, 2024. 2, 3, 6, 7
- [23] Pin-Hao Huang, Han-Hung Lee, Hwann-Tzong Chen, and Tyng-Luh Liu. Text-guided graph neural networks for referring 3d instance segmentation. *AAAI*, 35(2):1610–1618, 2021. 6
- [24] Ayush Jain, Nikolaos Gkanatsios, Ishita Mediratta, and Katerina Fragkiadaki. Bottom up top down detection transformers for language grounding in images and point clouds, 2021. 6, 7
- [25] Krishna Murthy Jatavallabhula, Alihusein Kuwajerwala, Qiao Gu, Mohd Omama, Tao Chen, Alaa Maalouf, Shuang Li, Ganesh Iyer, Soroush Saryazdi, Nikhil Keetha, et al. Conceptfusion: Open-set multimodal 3d mapping. *arXiv preprint arXiv:2302.07241*, 2023. 3
- [26] Li Jiang, Shaoshuai Shi, and Bernt Schiele. Open-vocabulary 3d semantic segmentation with foundation models. In *CVPR*, pages 21284–21294, 2024. 3

- [27] Xueying Jiang, Lewei Lu, Ling Shao, and Shijian Lu. Multimodal 3d reasoning segmentation with complex scenes. *arXiv preprint arXiv: 2411.13927*, 2024. 2, 3
- [28] Weitai Kang, Mengxue Qu, Jyoti Kini, Yunchao Wei, Mubarak Shah, and Yan Yan. Intent3d: 3d object detection in rgb-d scans based on human intention. *arXiv preprint arXiv:2405.18295*, 2024. 5, 6, 7
- [29] Amrin Kareem, Jean Lahoud, and Hisham Cholakkal. Paris3d: Reasoning-based 3d part segmentation using large multimodal model. In *ECCV*, pages 466–482. Springer, 2024. 3
- [30] Alexander Kirillov, Eric Mintun, Nikhila Ravi, Hanzi Mao, Chloe Rolland, Laura Gustafson, Tete Xiao, Spencer Whitehead, Alexander C Berg, Wan-Yen Lo, et al. Segment anything. In *ICCV*, pages 4015–4026, 2023. 3
- [31] Xin Lai, Zhuotao Tian, Yukang Chen, Yanwei Li, Yuhui Yuan, Shu Liu, and Jiaya Jia. Lisa: Reasoning segmentation via large language model. In *CVPR*, pages 9579–9589, 2024. 2, 3
- [32] Boyi Li, Kilian Q Weinberger, Serge Belongie, Vladlen Koltun, and René Ranftl. Language-driven semantic segmentation. *arXiv preprint arXiv:2201.03546*, 2022. 3
- [33] Haotian Liu, Chunyuan Li, Yuheng Li, and Yong Jae Lee. Improved baselines with visual instruction tuning. In *CVPR*, pages 26296–26306, 2024. 3
- [34] Yinhan Liu, Myle Ott, Naman Goyal, Jingfei Du, Mandar Joshi, Danqi Chen, Omer Levy, Mike Lewis, Luke Zettlemoyer, and Veselin Stoyanov. Roberta: A robustly optimized bert pretraining approach. *arXiv preprint arXiv:1907.11692*, 2019. 7
- [35] Youquan Liu, Lingdong Kong, Jun Cen, Runnan Chen, Wenwei Zhang, Liang Pan, Kai Chen, and Ziwei Liu. Segment any point cloud sequences by distilling vision foundation models. *NeurIPS*, 36:37193–37229, 2023. 3
- [36] Shiyang Lu, Haonan Chang, Eric Pu Jing, Abdeslam Boularias, and Kostas Bekris. Ovir-3d: Open-vocabulary 3d instance retrieval without training on 3d data. In *Conference on Robot Learning*, pages 1610–1620. PMLR, 2023. 3, 6
- [37] Yuhang Lu, Qi Jiang, Runnan Chen, Yuenan Hou, Xinge Zhu, and Yuexin Ma. See more and know more: Zero-shot point cloud segmentation via multi-modal visual data. In *ICCV*, pages 21674–21684, 2023. 3
- [38] Songyou Peng, Kyle Genova, Chiyu Jiang, Andrea Tagliasacchi, Marc Pollefeys, Thomas Funkhouser, et al. Openscene: 3d scene understanding with open vocabularies. In *CVPR*, pages 815–824, 2023. 3
- [39] Zhangyang Qi, Zhixiong Zhang, Ye Fang, Jiaqi Wang, and Hengshuang Zhao. Gpt4scene: Understand 3d scenes from videos with vision-language models. *arXiv preprint arXiv:2501.01428*, 2025. 2
- [40] Alec Radford, Jong Wook Kim, Chris Hallacy, Aditya Ramesh, Gabriel Goh, Sandhini Agarwal, Girish Sastry, Amanda Askell, Pamela Mishkin, Jack Clark, et al. Learning transferable visual models from natural language supervision. In *ICML*, pages 8748–8763, 2021. 3
- [41] Hanoona Rasheed, Muhammad Maaz, Salman Khan, and Fahad S. Khan. Llava++: Extending visual capabilities with llama-3 and phi-3, 2024. 7
- [42] Zhongwei Ren, Zhicheng Huang, Yunchao Wei, Yao Zhao, Dongmei Fu, Jiashi Feng, and Xiaojie Jin. Pixellm: Pixel reasoning with large multimodal model. In *CVPR*, pages 26374–26383, 2024. 3
- [43] Guangyan Sun, Mingyu Jin, Zhenting Wang, Cheng-Long Wang, Siqi Ma, Qifan Wang, Tong Geng, Ying Nian Wu, Yongfeng Zhang, and Dongfang Liu. Visual agents as fast and slow thinkers. *arXiv preprint arXiv:2408.08862*, 2024. 3
- [44] Hugo Touvron, Louis Martin, and Kevin Stone et al. Llama 2: Open foundation and fine-tuned chat models. *arXiv preprint arXiv: 2307.09288*, 2023. 7
- [45] Junchi Wang and Lei Ke. Llm-seg: Bridging image segmentation and large language model reasoning. In *CVPR*, pages 1765–1774, 2024. 3
- [46] Yanmin Wu, Xinhua Cheng, Renrui Zhang, Zesen Cheng, and Jian Zhang. Eda: Explicit text-decoupling and dense alignment for 3d visual grounding. In *CVPR*, pages 19231–19242, 2023. 5, 6, 7
- [47] Cilin Yan, Haochen Wang, Shilin Yan, Xiaolong Jiang, Yao Hu, Guoliang Kang, Weidi Xie, and Efstratios Gavves. Visa: Reasoning video object segmentation via large language models. In *ECCV*, pages 98–115. Springer, 2024. 3
- [48] Mi Yan, Jiazhao Zhang, Yan Zhu, and He Wang. Maskclustering: View consensus based mask graph clustering for open-vocabulary 3d instance segmentation. In *CVPR*, pages 28274–28284, 2024. 3
- [49] Jianing Yang, Xuweiyi Chen, Shengyi Qian, Nikhil Madaan, Madhavan Iyengar, David F Fouhey, and Joyce Chai. Llm-grounder: Open-vocabulary 3d visual grounding with large language model as an agent. In *ICRA*, pages 7694–7701. IEEE, 2024. 6
- [50] Jihan Yang, Runyu Ding, Weipeng Deng, Zhe Wang, and Xiaojuan Qi. Regionplc: Regional point-language contrastive learning for open-world 3d scene understanding. In *CVPR*, pages 19823–19832, 2024. 3
- [51] Chandan Yeshwanth, Yueh-Cheng Liu, Matthias Nießner, and Angela Dai. Scannet++: A high-fidelity dataset of 3d indoor scenes. In *ICCV*, 2023. 2, 5
- [52] Junbo Zhang, Runpei Dong, and Kaisheng Ma. Clip-fo3d: Learning free open-world 3d scene representations from 2d dense clip. In *ICCV*, pages 2048–2059, 2023. 3
- [53] Yiming Zhang, ZeMing Gong, and Angel X Chang. Multi3drefer: Grounding text description to multiple 3d objects. In *ICCV*, pages 15225–15236, 2023. 6
- [54] Chong Zhou, Chen Change Loy, and Bo Dai. Extract free dense labels from clip. In *ECCV*, pages 696–712. Springer, 2022. 3
- [55] Ziyu Zhu, Xiaojian Ma, Yixin Chen, Zhidong Deng, Siyuan Huang, and Qing Li. 3d-vista: Pre-trained transformer for 3d vision and text alignment. In *ICCV*, pages 2911–2921, 2023. 2, 7
- [56] Xueyan Zou, Jianwei Yang, Hao Zhang, Feng Li, Linjie Li, Jianfeng Wang, Lijuan Wang, Jianfeng Gao, and Yong Jae Lee. Segment everything everywhere all at once. *NeurIPS*, 36:19769–19782, 2023. 3